

PRESERVING BEAM QUALITY IN LONG RFQS ON THE RF SIDE: VOLTAGE STABILIZATION AND TUNING

Antonio Palmieri INFN-LNL, Legnaro (PD), Italy

Abstract

RFQs are the injectors customarily used in modern linacs and the achievement of a high beam transmission for a RFQs is of paramount importance in case of both high intensity linacs and RIBs facilities. This calls for an accurate control of the longitudinal inter vane voltage along the four structure quadrants (field stabilization), in order to keep its deviation from nominal value as low as possible (a few %, typically). In particular, for long RFQs (in which the structure length can be significantly higher than the RF wavelength), this aspect is more challenging, since the effect of a perturbation (e.g. due to mechanical errors and/or misalignments) on the nominal RFQ geometry has a major impact on voltage. This paper describes and analyses these issues, as well as the methods used to tackle them.

INTRODUCTION

In some important cases, the achievement of a high beam transmission (>95%) for a RFQ is a key issue for the proper operation of the overall facility in which the RFQ is included. This is particularly true in the cases of high intensity proton and/or deuteron RFQs (avg. beam power > 10 kW) and in the case of RIB acceleration. In the first case, the high space charge at low energy induces beam losses giving rise to the structure activation with the production of neutrons, (p-Cu and d-d reactions), and the loss control has to be compliant with a hands-on maintenance of the machine. In the second case, the RIB current loss can jeopardize the quality of the outcomes of Nuclear Physics experiments, while lost RIBs in the RFQ can give rise to high-lifetime decay products, which can undergo implantation reactions in the RFQ body.

These circumstances call for the adoptions of some adjustments in beam dynamics design and some stricter constraints on mechanical and electromagnetic parameters.

One of the adjustments is the accurate control of the longitudinal behavior of the inter-vane voltage along the four quadrants of the structure, and of voltage disuniformities among the quadrants with deviations from the nominal values that shall not exceed a few %. For instance, the following table lists these constraints for the RFQs being developed at LNL, namely the IFMIF RFQ [1], the TRASCO RFQ [2] and the SPES RFQ [3]. All of these RFQs have been designed for CW operation.

Table 1: RFQs Developed at LNL: Main Parameters

	TRASCO	IFMIF	SPES
status	Constructed	Construction in progress	Developing
f [MHz]	352.2	175	80
l [m]	7.13	9.8	7.2
R ₀ [mm]	2.93-3.07	4.13-7.10	5.27-7.86
ρ/R ₀	1	0.75	0.76
I _b [mA]	30	125	1e-6
V[kV]	68	79-132	64-86
W [MeV/u]	5	5	0.727
E.M. segments	3	1	1
Mech. modules	6	18	6
dV/V range	±1%	±2%	±3%
Q ₀	8000 (20% margin)	12000 (25% margin)	16000 (20% margin)
RF power [kW]	800 (20% margin)	1250(25% margin)	120(20% margin)

In order to understand the causes of these voltage deviations, it should be pointed out that the effect of a perturbation (e.g. due to mechanical errors and/or misalignments) on the nominal geometry in a four-vane RFQ provokes a mixing of the operating TE₂₁₀ mode (Quadrupole mode) with neighboring quadrupole TE_{21n} and TE_{11n} dipole modes. Now, if the overall RFQ length l is significantly greater than the wavelength λ, the eigenfrequencies f_n of the neighbouring modes can be very close to the operational one, i.e. f₀, thus enhancing the perturbation effect. The measures that are undertaken to tackle this issue consist in the “stabilization” and “tuning”. In particular, the RFQ stabilization involves actions that can be taken before knowing the actual RFQ voltage profile (i.e. in the design phase), namely: 1) The usage of coupling elements (resonant coupling) [4] this method consists in dividing the RFQ in N resonantly coupled segments and has the advantage of increasing the frequency spacing between the f₀ and the frequencies of the other quadrupole modes. This method is used mainly in RFQs with L/λ > 6 [5, 6, 7], 2). The usage of stabilizing devices for the dipole modes (dipole stabilizers or DSRs) [8]: this method consists in inserting longitudinal bars in the RFQ volume in correspondence of the end-cells and coupling cells, which do not perturbate

the quadrupole mode, but shift the dipole frequencies and create a “dipole-free region in the neighbourhood of the f_0 frequency. The RFQ tuning, indeed, consists in those actions that, starting from the actual knowledge of the voltage along z , and of the frequency in the real RFQ (typically by measurements), allow the attainment of the voltage specifications at the target frequency. In the following, this aspect will be analyzed in detail. The analysis will be carried out for four-vane RFQs only, and in particular for the RFQs developed at LNL.

RFQ CIRCUIT MODELING

A four vane RFQ can be modelled with a five conductor (the four electrodes E1, E2, E3 and E4 plus a “virtual” ground) transmission line, whose infinitesimal element of length dz is shown in Figure 1[9]. This topology is similar to the four-conductor line used in [10]. In such circuit the L_{si} ($i=1,\dots,4$) are the inductances associated with the longitudinal current flow along the vanes, L_i and C_i are respectively the inductances (integrated in length) associated with the flux of magnetic field through the RFQ cross-section and the intra-vane capacitances (per unit length). C_a and C_b are the capacitances (per unit length) between opposite vanes.

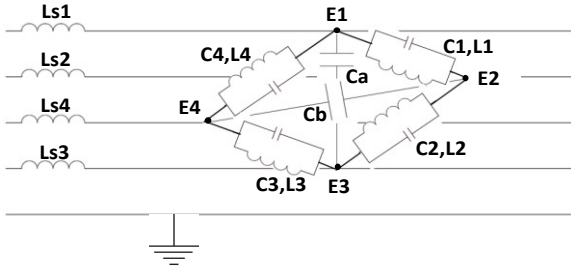


Figure 1: The RFQ equivalent transmission line.

In the ideal RFQ ($C_i=C$, $L_i=L$ and $C_a=C_b$, $i=1,\dots,4$), by defining $\omega_0^2=1/LC$ and $h=C_a/C$, the line equations can be written as follows, where U_i are the inter-vane voltages ($U_i=E_{(i \bmod 5)+1}-E_i$).

$$\frac{d^2 \underline{U}}{dz^2} = \left(-\frac{\omega^2}{c^2} + \frac{1}{c^2} \underline{C}^{-1} \underline{L} \right) \underline{U} \quad (1)$$

Here $\underline{A} = \underline{C}^{-1} \underline{L}$ is a 4x4 circulant matrix defined by the vector $\underline{\Omega} = (\omega_0^2/4)[1+2/(1+h), -1, -(1-h)/(1+h), -1]$. The eigenvalues of \underline{A} are proportional to the quadrupole TE_{21} and dipole TE_{11} frequencies ($f_q = f_0$ and $f_d = f_0 / \sqrt{1+h}$), plus a zero eigenvalue corresponding to the “monopole mode” the only goal of which is to guarantee the voltage consistence of $U_1+U_2+U_3+U_4=0$. A transformation between modal voltage vector $\hat{\underline{U}} = U_q \hat{e}_q + U_m \hat{e}_m + U_{d1} \hat{e}_{d1} + U_{d2} \hat{e}_{d2}$ and vane voltage vector \underline{U} is therefore established. Moreover, this transformation decouple the transmission line in three independent equivalent lines, corresponding to the Q and the two D modes, with longitudinal wave number

$\gamma = (1/c)\sqrt{\omega^2 - \omega_c^2}$ where ω_c can be ω_q or ω_d . If boundary conditions for the RFQ $U'(0)=U'(l)=0$ @ $f=f_0$ are assigned via a resonant lumped LC element (End-cell) [8], longitudinal quadrupole and dipole eigenfrequencies $f_{q0}, f_{q1}, \dots, f_{qn}, \dots, f_{d0}, f_{d1}, \dots, f_{dn}, \dots$ and orthonormal eigenvectors $\underline{\phi}_{qn} = \phi_{qn} \hat{e}_1, \underline{\phi}_{d1n} = \phi_{dn} \hat{e}_3, \underline{\phi}_{d2n} = \phi_{dn} \hat{e}_4, n \in N_0$ can be determined.

PERTURBATION ANALYSIS

In case of geometric errors in the RFQ vane and/or vessel profiles, a perturbative term $\underline{\delta A}$ appears. From the purely geometrical point of view, this term is due to capacitance perturbations $\underline{\delta C}$ (i.e. due to mean aperture R_0 deviations from the nominal value) and/or inductance perturbations $\underline{\delta L}$ (i.e. electrode height H or tank radius deviations). In this case, the perturbed operator reads

$$\underline{\delta A} = c^{-2} \delta(\underline{C}^{-1} \underline{L}) = c^{-2} (\underline{C}^{-1} \underline{\delta L} - \underline{C}^{-1} \underline{\delta C} \underline{A})$$

and, in the modal basis,

$$\underline{\delta k}^2 = c^{-2} \underline{S}^{-1} \underline{C}^{-1} (\underline{\delta L} - \underline{\delta C} \underline{A}) \underline{S}$$

\underline{S} being the eigenvector matrix. Therefore it is possible to write the explicit expression of the perturbed voltage of the RFQ as follows: $\underline{U} = U_0 \underline{\phi}$, with

$$\underline{\phi} = \underline{\phi}_{q0} + \delta \underline{\phi} = \underline{\phi}_{q0} + \sum_{n=1}^{\infty} a_{qn} \underline{\phi}_{qn} + \sum_{n=0}^{\infty} a_{d1n} \underline{\phi}_{d1n} + \sum_{n=0}^{\infty} a_{d2n} \underline{\phi}_{d2n}$$

where

$$a_{qn} = \frac{-\omega_0^2}{4(\omega_0^2 - \omega_{qn}^2)} \int_0^l \phi_{q0} \phi_{qn} \left(\frac{\delta C_{QQ}}{C} + \frac{\delta L_{QQ}}{L} \right) dz \quad n \in N$$

$$a_{d1n, d2n} = \frac{-\sqrt{2}\omega_0^2}{4(\omega_0^2 - \omega_{dn}^2)} \int_0^l \phi_{q0} \phi_{dn} \left(\frac{\delta C_{Qd1, Qd2}}{C} + \frac{\delta L_{Qd1, Qd2}}{L} \right) dz \quad n \in N_0$$

with

$$\delta C_{QQ} = \sum_i \delta C_i, \quad \delta L_{QQ} = \sum_i \delta L_i$$

$$\delta C_{Qd1} = \sqrt{2}(\delta C_1 - \delta C_3) / (1+h), \quad \delta C_{Qd2} = \sqrt{2}(\delta C_4 - \delta C_2) / (1+h)$$

$$\delta L_{Qd1} = \sqrt{2}(\delta L_1 - \delta L_3), \quad \delta L_{Qd2} = \sqrt{2}(\delta L_4 - \delta L_2)$$

The perturbed quadrupole frequency is:

$$\Delta \omega_0 \cong -c^2 / 2\omega_0 \left\langle \hat{\underline{U}}_{q0} \left| \underline{\delta k}^2 \right| \hat{\underline{U}}_{q0} \right\rangle.$$

The term $(\omega_0^2 - \omega_n^2) / \omega_0^2$ is proportional to $(\lambda/l)^2$ and therefore, the longer the RFQ, the more important is the perturbation effect. Moreover, it is evident that a key parameter is the dependence of the δL 's and δC 's on the geometric errors in the RFQ, which cause a variation of the local cut-off frequency f_0 for the Q mode $\delta f_0 = -(1/2)(f_0/C)\delta C + 1/2(f_0/L)\delta L$. In particular, it has to be taken into account that the C depend mainly on R_0 and ρ , while L depend mainly on the upper RFQ wall height (or tank radius) H and on the electrode thickness W_b .

Therefore it is possible to write that $\delta C_i = \alpha_{R0} \delta R_0 + \alpha_\rho \delta \rho$ and $\delta L_i = \alpha_H \delta H + \alpha_{Wb} \delta W_b$, and equivalently that $\delta f_0 = \chi_{R0} \delta R_0 + \chi_\rho \delta \rho + \chi_H \delta H + \chi_{Wb} \delta W_b$. On the other hand, it should be observed that, while χ_ρ depends only on

construction accuracy ($\pm 10\text{-}20\ \mu\text{m}$ is the state of the art), χ_{R0} depends on electrode positioning (errors of $\pm 100\ \mu\text{m}$ can occur), due to alignment and/or brazing. As for the inductive terms, their sensitivities χ_H and χ_{wb} turn out to be one order of magnitude lower than the corresponding capacitive ones. These parameters, obtained via 2D and 3D simulations are listed in Table 2.

Table 2: Frequency Sensitivities W/O Geometric Deviations for the RFQs Developed at LNL (per Quadrant)

	TRASCO	IFMIF	SPES
χ_{R0} [MHz/mm]	40	7.6 to 11.8	2.7 to 3.5
χ_p [MHz/mm]	-30	-3.6 to 7-5.3	-3.2 to -2.2
χ_H [MHz/mm]	-3.2	-0.9	-0.13
χ_{wb} [MHz/mm]	2.0	0.55	0.16

With these values it is possible to analyze the effect of a perturbation on the quadrupole TE_{210} voltage profile. As a first example, the misalignment of one electrode will be considered on a 9.9 m un-segmented RFQ with constant U and R_0 operating at 175 MHz with ideal boundary conditions for the Q mode with $\chi_{R0}=7.6$ MHz/mm. In particular, in case one electrode is displaced of $\delta R_0=0.05$ mm away from beam axis for all z in the interval $[a, l/2+a]$ with respect to its nominal position and with a varying in the interval $[0, l/2]$, a corresponding perturbation of the capacitances C_1 and C_4 occurs. As expected, the perturbed voltages are proportional to ΔR_0 and the Q component scales as $(\lambda/l)^2$. The diagram is shown in Figure 2 for the case of Q and D components.

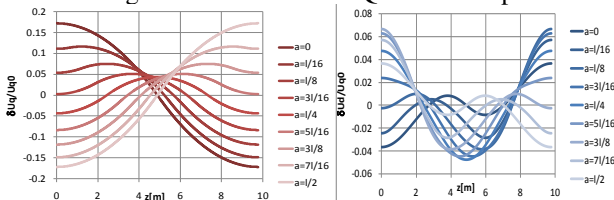


Figure 2: The voltage perturbations (Q component, left, D component, right).

Already from this example it is possible to notice that, only with electrode misalignments in the order of tenth of μm , the voltage specifications are not met, and the RFQ stabilization mechanisms alone are not able to meet the requirements.

TUNERS AND TUNING RANGE

In order to meet the requirements, it is necessary to use a system of N_T slug tuners per quadrant. Tuners are metallic cylinders of radius a placed on the upper walls of the RFQ and inserted for a depth h in the cavity volume, which compensate the geometric variation in capacitive region with corresponding variations in the inductive region. Figure 3 shows the tuners for the TRASCO RFQ.

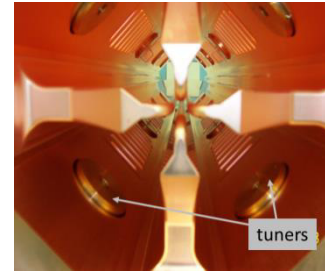


Figure 3: Tuners inserted in the TRASCO RFQ.

A tuner placed in the position z_i ($i=1,\dots,NT$) varies both the local cut-off frequency for any z in the interval

$[z_i-a, z_i+a]$, and global resonant frequency according to the relationships (for $h>0$)

$$\delta f_{q0}(z_i) = \chi_{i2D} h_i \quad \delta f_0 = \chi_{3D} h$$

Therefore, if the function $\delta f_{q0j}(z) \sim -1/2 \delta C_j(z)/C$, ($j=1,\dots,4$) is known, by setting the tuner heights h_i in such a way that $\delta L_j(z_i) = -(L/C) \delta C_j(z_i)$ it is possible to compensate the capacitance and therefore the voltage perturbation. The basic idea is that the tuning range (the frequency interval that can be spanned by the tuners) defined as $\Delta f_{TR} = 4N_T \chi_{3D}(h_1+h_2)$, should correct frequency (local and global) shifts induced by the maximum δR_0 error to be expected. It should be noticed that, since the overall frequency perturbation is due to terms coupled with operating mode, it is not compensated by the previous relationships. As an empiric rule, half of the tuning range is employed for f_0 correction and the other half for voltage correction. Typically, the tuning range is expected to be symmetric about the operational frequency f_0 , i.e. $\Delta f_{TR} = [f_0 - \Delta f_{TR}/2, f_0 + \Delta f_{TR}/2]$ corresponding to $[0, h_1+h_2]$. This is due to the fact that, if $h<0$, the tuner sensitivity decays exponentially. In particular, this implies that f_0 is higher than the average cut-off frequency for the TE_{210} mode of the RFQ f_{q0} of an amount equal to $\Delta f_{TR}/2$.

An unwanted but unavoidable effect of tuners is the increase in power consumption. An estimation of such effect can be done by considering the case of maximum h_1+h_2 and calculating the dissipated power on the tuners ΔP (with a factor 2 safety margin). This extra power has to be considered when dimensioning the RF system, too. Table 3 lists a comparison for the tuning ranges of the RFQs developed at LNL.

Table 3: Tuning Ranges for the RFQs

	TRASCO	IFMIF	SPES
NT	96	88	96
a [mm]	24.5	44.5	44.5
ΔR_0 range [mm]	± 0.05	± 0.1	± 0.2
Δf range [MHz]	± 1	± 1	± 0.5
h_1+h_2 range [mm]	[-10, 10]	[-15, 30]	[0, 80]
$\Delta P/P_0$ [%]	4	7	8

PERTURBATION SYNTHESIS AND TUNING ALGORITHM

The basic idea of perturbation synthesis is that the capacitance (or inductance) perturbative terms can be spanned in series of the quadrupole and dipole eigenfunctions ϕ_{qm} and ϕ_{dm} . Therefore, coefficients b_{qm} , $b_{d1m,d2m}$ exist such that:

$$\delta C_{QQ} = \sum_{m=1}^{NQ} b_{qm} \phi_{qm}, \delta C_{Qd1,Qd2} = \sum_{m=0}^{Nd1,Nd2} b_{d1m,d2m} \phi_{dm}$$

where NQ , $Nd1$ and $Nd2$ are the number of harmonics used. Now, provided that the measured perturbed components ΔU_q , U_{qd1} and U_{qd2} can be spanned in series of RFQ eigenfunctions as follows,

$$a_{qn} = \int_0^1 \Delta U_q \phi_{qn} dz, n \in N, a_{d1n,d2n} = \int_0^1 U_{qd1,qd2} \phi_{dn} dz, n \in N_0$$

The substitution of the above expression in the perturbative voltage development leads to the following matrix equations, from which the unknown coefficient b_{qm} , $b_{d1m,d2m}$ can be obtained

$$C^{(q)} b_q = a_q, C^{(d)} b_{d1} = a_{d1}, C^{(d)} b_{d2} = a_{d2}$$

The $N_T \times 4$ matrix δh of tuner heights can be transformed into the modal function basis, thus obtaining the three vectors of N_T elements $\delta h_Q, \delta h_{d1}, \delta h_{d2}$. Such vectors can be multiplied by appropriate gain parameters g_Q, g_{d1} and g_{d2} , in order to speed up the tuning convergence process. For example, let us consider the case of the SPES RFQ with two electrodes displaced of 0.2 mm, $R_0=5.8$ mm, $\chi_{R0}=3.5$ MHz/mm. This leads to a frequency shift of 150 kHz and Q [D] perturbations on nominal voltage of $\pm 10\%$ [$\pm 20\%$]. With the usage of 24 regularly spaced tuners per quadrant ($\Delta z_T=l/24$), the tuning algorithm is implemented with $g_Q=g_{d1}=g_{d2} 3.5$, $N_q=N_d=2$. In this case, the tuner depth profiles which reduce all perturbative components within $\pm 2\%$ are shown in Figure 3. The tuning range is able to compensate the effect of such perturbation, but, at the same time, it saturates for $z < 2m$. This is an indication of the relationship between the δR_0 and $h1+h2$ ranges.

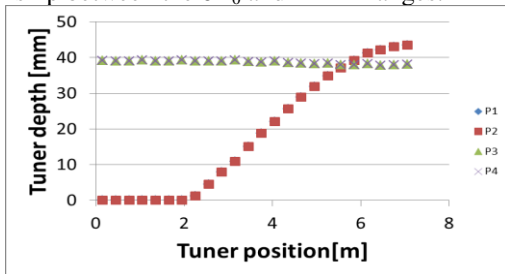


Figure 4: Tuner depths vs position for SPES RFQ (test case).

Due to the discreteness of tuner positions, the tuning procedure scheme is iterative and some iterations are needed in order to converge up to the attainment of the specifications. The tuner spacing should be kept as uniform as possible although, in principle, tuner periodicity is broken by the presence of vacuum ports,

couplers etc. In fact, if the same exercise of Figure 4 is repeated for a set of tuners spaced in six groups of four tuners with $\Delta z_T=l/48$, and with a tuner free zone of $5l/48$ between each set, the Q component lies within $\pm 4\%$ with the same tuner height range.

An interesting spin-off of this analysis consists in the identification of the water variation temperature to be applied to the RFQ vessel in case of a detuning during high power operations. The RFQ frequency is controlled by varying the temperature difference between vanes and vessel $T-T_v$. Now, if one of the two temperatures (i.e. vane) is kept constant and N independent cooling circuits are foreseen for the vessel, each l/N long subdivision of the RFQ can act as a tuner. The case of IFMIF RFQ, with $N=3$ (3 supermodules) $T_v=15^\circ C$, $\partial f/\partial(T-T_v)=16kHz/^\circ C$, $T=22^\circ C$ is an example. Let us suppose that some detuning occurs due to thermal-induced deformation at RFQ extremities ($\Delta R_0=0.1$ mm to 0 mm in the first and last 20 cm of the cavity): such effects were observed for instance in the High Power Testing of TRASCO RFQ. In Figure 5 it is possible to see the comparison between untuned and tuned voltage: the temperature variations needed to tune the voltage were $+0.9^\circ C$ in Supermodules 1 and 3 and $-1.8^\circ C$ in Supermodule 2.

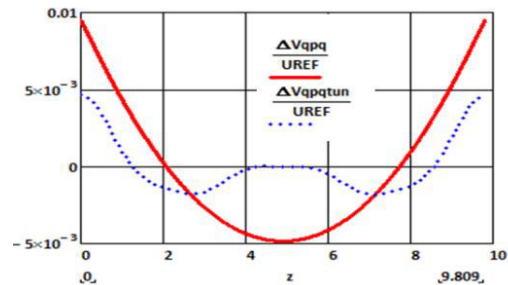


Figure 5: Estimation of Voltage tuning with water temperature variation: untuned [tuned] $\delta U_q/U_{q0}$ (solid curve) [(dotted curve)].

EXPERIMENTAL RESULTS

The methods described in this paper were experimentally tested on the TRASCO and IFMIF RFQs. In particular, the following set-ups were measured: 1) The first 2.36 m module of the TRASCO RFQ, used for high power testing [2], 2) the 9.9 m full-scale aluminium model of the IFMIF RFQ [11,12], and 3) the 2m IFMIF RFQ (3 modules (16th, 17th and 18th) out of 18 + 1 39 cm RF plug) to be used for the High Power tests. The functions $U_i(z)$ were measured with the Bead Pulling technique, with dielectric bead in case 1), magnetic bead in case 3) and both in case 2). If a metal bead is used, the presence of the tuners strongly affects the phase acquisition. Therefore, the raw phase data need to be properly interpolated in order to get rid of the tuner-induced bumps. The available tunable dummy devices are: a) Tunable end-cell: the proper boundary condition is obtained by varying the end-plate thickness, b) Tunable DSRs (case 1 only): the attainment of the dipole-free

region is obtained by varying the length of the rods at both RFQ ends (Figure 6), c) Dummy aluminium tuners.

The initial step in the tuning consists of experimentally determining the optimum thickness of the End Cell and DSR lengths. The tuning algorithm is then applied to the dummy tuners. Finally, the coupling dummy loop(s) is included in order to verify its effects on the voltage uniformity and final end plates are mounted: copper tuners are machined to length and replaced in batches (4 batches in case 1, and 3 batches in case 3), in order to perform minor correction to the tuner heights if needed (Figure 7).

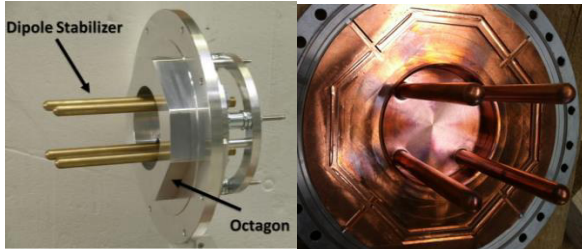


Figure 6: Tunable (left) and final (right) end cell equipped with DSRs used for the TRASCO RFQ High Power Tests. The inserted thickness of the end plate (octagon) is visible.

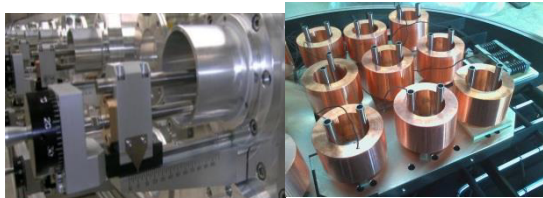


Figure 7: Dummy (left) and copper tuners brazed and to be machined to length (right) for the IFMIF RFQ.

The results of tuning procedure are summarized in Table 4. In particular, it should be considered that the tuning results in the 3rd column do not include the RF plug.

Table 4: Summary of Tuning Procedures

	TRASCO	IFMIF AI model	IFMIF High Power test
Tuner heights	[-4.8,11.5]	[11.2, 18.2]	[-14.7, 12.2]
$\delta U_q/U_0$ [%]	+12/-15	-21/+22	-8/+3
untuned (tuned)	(± 1)	(± 2)	(-0.5,+1.0)
U_{qd1}/U_0 [%]	-10/+4	± 3	-0.3/+0.9
untuned (tuned)	(± 1)	(± 2)	(0, 0.8)
U_{qd2}/U_0 [%]	-7/+17	-1/+3	0.3/0.9
untuned (tuned)	(-1/+2)	(± 2)	(0.2/0.8)

Here, “untuned” means that all the tuners were set at half of their range. In the case of IFMIF AI model, the fact that the tuners are not regularly spaced provokes the large perturbation for the Q mode. Fig. 8 shows the comparison between measured voltage $\Delta U_q/U_0$ (red curve) and the same quantity obtained with perturbative

analysis (blue curve), in the untuned case for the IFMIF RFQ Aluminium model.

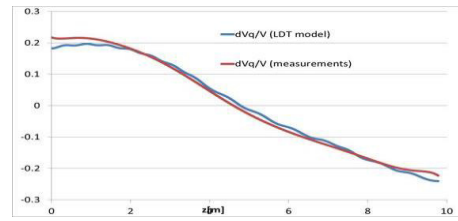


Figure 8: $\delta U_q/U_0$: measured data (red curve) vs Perturbation Analysis forecasts (blue curve).

Finally, Figure 9 shows the final tuning results for the TRASCO and IFMIF High Power Test RFQs.

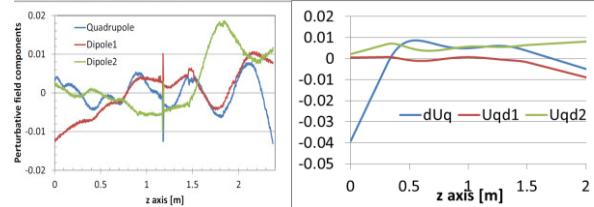


Figure 9: $\delta U_q/U_0$ obtained for TRASCO (left) and IFMIF (right) RFQs.

CONCLUSIONS AND PERSPECTIVES

The analysis proved useful in the design phase of the RFQ. The identification of the needed tuning margins and experimental results confirmed the adopted approach. The next steps include the tuning of the final structures considered in this paper and the analysis on the effects of “real” RFQ voltage profile on beam dynamics parameters.

ACKNOWLEDGMENTS

The author wishes to acknowledge all the people that were involved in this work, namely Dr. Andrea Pisent, Dr. Michele Comunian, Dr. Enrico Fagotti, Dr. Francesco Grespan, and all the engineers and technicians of INFN-LNL, INFN-Padua and INFN-Turin who arranged the setup and made the RF measurements possible.

REFERENCES

- [1] M. Comunian, A. Pisent, IPAC 2011 p.670
- [2] E. Fagotti et al, LINAC 2012, p.828
- [3] M. Comunian et al. LINAC 2012, p. 951
- [4] L. Young, LINAC 90, p.530
- [5] L. Young et al., LINAC 98 p.270
- [6] E. Fagotti et al., LINAC 2008
- [7] O. Piquet et al., IPAC 2014
- [8] F. Grespan et al., Nuclear Instruments and Methods in Physics Research A 582 (2007) 303–317
- [9] A. Palmieri et al, IPAC 2010 p. 606.
- [10] A. France, IPAC 2014 p. 34
- [11] A. Palmieri et al, IPAC 2010 p. 609.
- [12] A. Palmieri et al, LNL Annual Report 2012